Ordered Nanostructures

1D Arrangement of Au Nanoparticles by the Helical Structure of Schizophyllan: A Unique Encounter of a Natural Product with Inorganic Compounds**

*Ah-Hyun Bae, Munenori Numata, Teruaki Hasegawa, Chun Li, Kenji Kaneko, Kazuo Sakurai, and Seiji Shinkai**

Assemblies of inorganic materials on the nanoscale have received considerable attention in recent years owing to their potential use as novel functional materials.[1] Especially, arrangement of metal nanoparticles in desired assemblies may be a new methodology for nanopatterning, which is indispensable for nanotechnologies. However, it is difficult to create assemblies of metal particles in a regulated fashion because of their inability to self-assemble without the aid of organic molecules. One approach to overcome these difficulties includes the immobilization of the metal with organic molecules or polymers to yield two- or three-dimensional organic–metal hybrid nanostructures in which the metal particles are linked by the organic molecules.[2] For example, several research groups have successfully exploited biological macromolecules such as DNA and antibodies to create metal assemblies in which DNA–DNA or antibody–antigen interactions play a crucial role in the self-assembling process of the inorganic nanoparticles.[3]

The preparation of a one-dimensional metal array in the solution state is a fascinating target owing to favorable electronic and magnetic properties which may result from their alignment and allow application of the arrays as nanowires or nanosensors. However, to arrange metal particles into a 1D array requires a sophisticated approach because otherwise the metal surface tends to aggregate into two- or three-dimensional structures. Bioinorganic nanocomposite materials based on metal nanoparticles and 1D biomolecular species, namely DNA[4] and proteins,[5] have recently attracted considerable interest because of the potential to tune the optical, electrical, and even mechanical properties of these materials.[6] For example, Shionoya and coworkers[7] successfully aligned a metal array in one dimension by using a double-stranded skeleton of DNA that contained metal-coordination moieties. However, successful examples of 1D metal arrays in solution are still very limited.

Schizophyllan (SPG) is a natural polysaccharide produced by the fungus *Schizophyllum commune*, and its repeating unit consists of three β-(1–3)-glucoside and one β-(1–6)-glucoside side chain linked at every third main-chain glucoside unit (Figure 1). Interestingly, SPG adopts a triple-helical conformation (t-SPG) in nature which is stabilized by hydrogen-bonding interactions between 2-hydroxy groups, but can be dissociated (reversibly) into a single chain (s-SPG) by dissolving it in dimethylsulfoxide (DMSO);[8] the s-SPG chain can reassume the original triple-helix arrangement by exchanging DMSO for water. In the glucose unit, the 2-hydroxy side of the molecule is a hydrophobic face, whereas the 6-hydroxy side is a hydrophilic face.[9] As the triple-stranded helical structure of SPG is stabilized by the hydrogen-bonding interaction between the 2-hydroxy groups formed inside the helical column, one may presume that the inside hollow is considerably hydrophobic, in a similar fashion to the inside cavity of cyclodextrins.[10] It thus occurred to us that when the renaturating process from s-SPG to t-SPG is carried out in the presence of hydrophobic polymers or assemblies, they would be entrapped in the cavity with the aid of the hydrophobic force to give a novel nanocomposite, which has a unique one-dimensional structure. In this case, the inner cavity of t-SPG may be somewhat enlarged by the inclusion of a guest and as a result several hydrogen bonds may be cleaved, but this destabilization would be sufficiently compensated by the stabilization effect arising from the SPG–guest interaction. Previously, we focused our attention on the inclusion of single-walled carbon nanotubes and found that SPG can include them inside the helical structure through the renaturating process.[11] Herein our attention is focused on extending this novel concept to Au nanoparticles, and we report that owing to its strong helix-forming nature, SPG is capable of assembling Au nanoparticles into a one-dimensional array (Figure 2).

Stock solutions of s-SPG were prepared in DMSO or water. An aliquot of an aqueous solution of dispersed Au nanoparticles (250 μL containing 1250 particles of 5-nm diameter) was mixed with the solution of s-SPG (M_w = 150000) in DMSO (50 mg mL^{-1}, 50 μL). The mixture was centrifuged (9000 rpm) for 1 h, and the supernatant, which contained unconverted s-SPG and Au nanoparticles, was removed with a pipette. The precipitated SPG–Au complexes were separated and then dispersed into fresh water (200 μL). By repeating this process three times, any excess s-SPG was removed and the solvent was replaced by water. We found that both SPG and amylose yield a homogeneous aqueous solution in the presence of Au nanoparticles, whereas other polysaccharide samples (dextran and pullulan) result in a

[*] A.-H. Bae, Dr. M. Numata, Dr. T. Hasegawa, Dr. C. Li, Prof. Dr. S. Shinkai
Department of Chemistry and Biochemistry
Graduate School of Engineering
Kyushu University
Fukuoka 812-8581 (Japan)
Fax: (+81) 92-642-3611
E-mail: seijitcm@mbox.nc.kyushu-u.ac.jp
Prof. Dr. K. Kaneko
HVEM Laboratory
Kyushu University
Fukuoka 812-8581 (Japan)
Prof. Dr. K. Sakurai
Department of Chemical Processes and Environments
Faculty of Environmental Engineering
The University of Kitakyushu
1–1 Hibikino, Wakamatsu-ku, Kitakyushu
Fukuoka 808-0135 (Japan)

[**] We thank Taito Co., Japan, for providing schizophyllan samples. This work was supported by the Japan Science and Technology Corporation, SORST Program.

Supporting information for this article is available on the WWW under http://www.angewandte.org or from the author.

  DOI: 10.1002/ange.200462810

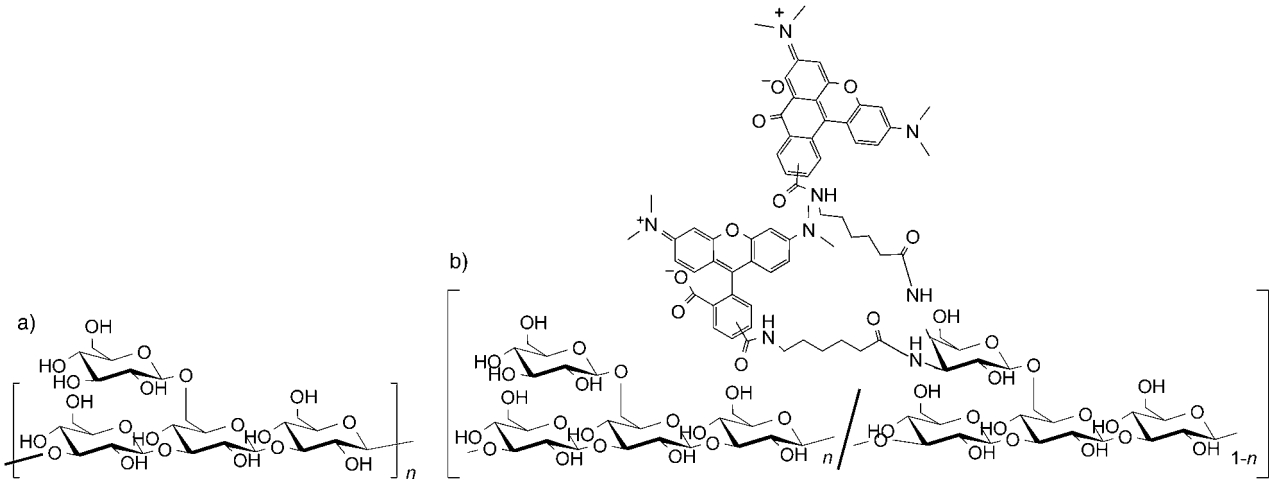

Figure 1. Repeating units of a) schizophyllan (SPG) and b) rhodamine-appended SPG (Rho-SPG).

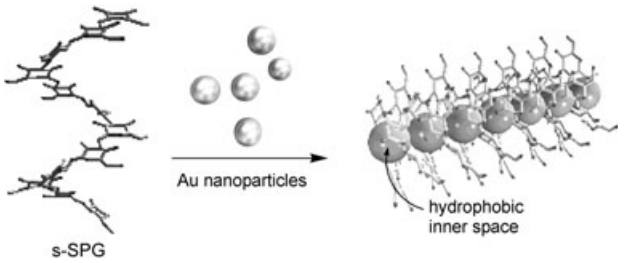

Figure 2. 1D array of Au nanoparticles resulting from their inclusion in the helical structure of SPG.

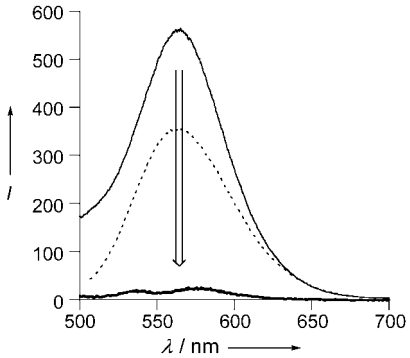

Figure 3. Fluorescence spectra of Rho-SPG (——) and the Rho-SPG–Au complex (——) in aqueous solution at 25 °C (λ_{ex} = 450 nm). Also shown is the reference spectrum of rhodamine dye in the presence of Au nanoparticles (-----).

precipitate. The SPG–Au complex was characterized by UV/Vis absorption spectroscopy. It is well known that Au nanoparticles show a plasmon absorption peak at 525 nm, which is significantly broadened upon aggregation.[12] In the present system, this peak was substantially broadened which indicates that the nanoparticles are assembled by s-SPG (see Supporting Information).

We further confirmed the formation of the composite between SPG and the Au nanoparticles by using rhodamine-appended SPG (Rho-SPG, see Figure 1) instead of s-SPG. The Rho-SPG–Au complex was prepared by an identical procedure to that used for the s-SPG–Au complex and then characterized by fluorescence spectroscopy. The fluorescence spectrum of Rho-SPG shows an emission peak at 565 nm, which is characteristic of rhodamine. However, the intensity of fluorescence of the dye in the Rho-SPG–Au complex was decreased to nearly zero (Figure 3). To examine whether the fluorescence of the dye was quenched by the metal nanoparticles themselves, we mixed Au nanoparticles and rhodamine and observed that there was no significant quenching of the fluorescence of the dye. This result suggests that the interaction of all three components—dye, nanoparticles, and SPG—leads to a decrease in the fluorescence of rhodamine, and supports the view that Au nanoparticles are entrapped by Rho-SPG.[13]

To obtain further evidence that SPG interacts with Au nanoparticles, the morphology of the complex was directly observed by AFM and TEM. By AFM, we observed the presence of fibrous structures of the complex, with diameters of around 6–7 nm, which are wider than that of SPG chains (≈1 nm, see Supporting Information). The Au nanoparticles have an average diameter of 5 nm. The coincidence of the diameter of the complex (≈6–7 nm) with the sum of the diameters of the nanoparticles and SPG (approximately 5 and 1 nm, respectively) supports the view that Au nanoparticles are arranged one-dimensionally through wrapping of SPG chains by hydrophobic force.[14] This unique morphology is probably a result of the inclusion of Au nanoparticles in the SPG helical structure. TEM images of Au nanoparticles on their own as well as in their complex with s-SPG are shown in Figure 4. The TEM pictures were taken without staining: the images shows the spots of Au nanoparticles themselves. From the TEM image shown in Figure 4a, we can see that Au nanoparticles are randomly distributed on the grid. On the other hand, in the presence of s-SPG, Au nanoparticles appear to be one-dimensionally aligned, which suggests that the wrapping by s-SPG enforces Au nanoparticles to adopt a 1D arrangement (Figure 4b). The length of the complex is consistent with that of s-SPG itself (≈200 nm). In reference

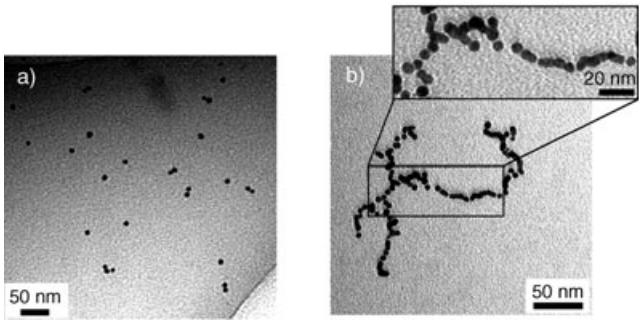

Figure 4. TEM images of a) Au nanoparticles and b) the SPG–Au complex, both in the absence of stain.

experiments, we prepared separate samples of amylose–Au (amylose: $M_w = 15000$) and t-SPG–Au complexes according to the same procedure. However, we could not recognize any significant structure as observed for the s-SPG–Au complex (see Supporting Information). From these TEM images, we can conclude that the difference in the higher-order morphology between SPG (highly ordered triple-helix) and amylose (random coil or disordered helix) determines the final characteristic structure of the complexes: that is, the strong helix-forming nature of SPG is the driving force to arrange Au nanoparticles in one dimension.

The presence of s-SPG in the complex was revealed by energy-dispersive X-ray (EDX) spectroscopy. Figure 5 shows a TEM image of the s-SPG–Au complex and its EDX line-scan profile. As seen in Figure 5, the oxygen component that arises from SPG overlaps the Au

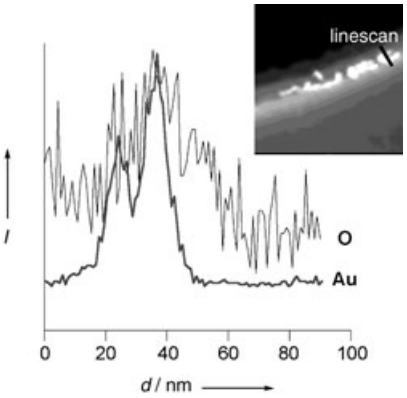

Figure 5. An EDX line-scan profile and TEM image of the SPG–Au complex; d = distance.

component and confirms the coexistence of these two elements. Furthermore, it should be emphasized that broadened distribution of the oxygen element in comparison to that of Au supports our assumption that Au nanoparticles are wrapped by SPG. The findings further confirm that s-SPG works as a "mold" for the one-dimensional arrangement of Au nanoparticles.

Furthermore, we succeeded in taking a three-dimensional image of this picture.[15] The four selected still pictures are shown in Figure 6b–e (see also Supporting Information), and each 3D image corresponds to the clockwise rotation of the structure shown in Figure 6a, with 45°, 135°, 225°, and 315° along a perpendicular axis. In these 3D images, one can see that SPG appears as a thin white layer around the Au

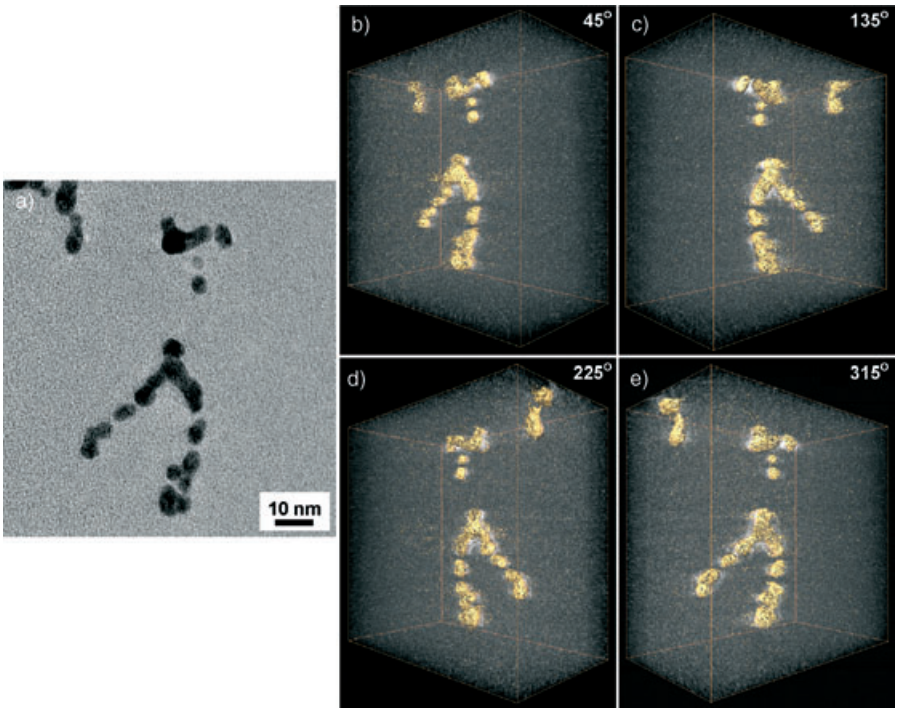

Figure 6. High-resolution 3D TEM images of the s-SPG–Au complex.

nanoparticles. This result strongly supports the fact that s-SPG can enwrap Au nanoparticles without any gaps and arrange them in a one-dimensional array.[16]

In conclusion, we have demonstrated that Au nanoparticles can be aligned in one-dimensional architecture by wrapping them in the helical structure of schizophyllan. The findings clearly show that schizophyllan has potential as an induced-fit-type one-dimensional host and implies many future applications not only to arrange Au nanowires in a desired orientation but also to assemble other hydrophobic building blocks. We believe, therefore, that this system would be readily applicable to the design of new sensors, nanocomposites, nanowires, and nanocircuits.

Experimental Section

Synthesis of rhodamine-appended SPG: Schizophyllan (500 mg, $M_w = 150000$) was suspended in distilled water (500 mL), and the

mixture was heated at reflux for 12 h until a clear solution was obtained. After cooling to room temperature, $NaIO_4$ (4.0 mg) was added and the mixture was stirred at 4 °C for 3 d protected from light by a shield. To remove inorganic salts, the resultant solution was subjected to dialysis with cellulose membrane (MWCO = 3500) to give an aqueous solution that contained aldehyde-appended SPG. Methylamine (1.0 mL of 40 % aqueous solution) and $NaBH_3CN$ (100 mg) were added to the resultant solution of SPG (500 mg of SPG), and the mixture was stirred at room temperature for 5 days. Dialysis with cellulose membrane followed by freeze–dry treatments gave amine-modified SPG as a white powder. The modification ratio was estimated by elemental analysis.

An excess amount of 6-(tetramethylrhodamine-5-(and 6)-carboamido) hexanoic acid succinimidyl ester (1.0 mg; Molecular Probes) was added to a solution (5.0 mL) in DMSO of methylamine-modified SPG (30 mg), and the mixture was stirred at room temperature in the dark. After one week, the resultant solution was dialyzed against distilled water through a cellulose membrane (MWCO = 3500). This dialysis process was repeated until the color of the tetramethylrhodamine no longer persisted in the distilled water, which indicated complete removal of any unreacted dye. Freeze–dry treatment of the resultant solution gave rhodamine-appended SPG (Rho-SPG) as a purple powder. The percentage of rhodamine introduced was determined by elemental analysis to be 3.0 mol %.

Au nanoparticles (5-nm diameter) were purchased as an aqueous solution of bare gold nanoparticles (without surfactant stabilizer; BB International). TEM and HR-TEM images were acquired using JEOL TEM-2010 (acceleration voltage: 120 kV) and FEI TECNAI-20 (acceleration voltage: 200 kV) apparatus, respectively. A TEM grid was dried under reduced pressure for 6 h before TEM observation. EDX spectra and EDX line-scan profiles were obtained using a FEI TECNAI-20 microscope. AFM images were acquired in air using a Topo METRIX SPM 2100 (noncontact mode). The sample was cast on mica and dried for 6 h under reduced pressure before AFM observation. 3D TEM images were taken using a FEI TECNAI-20 microscope. The TEM parameters were controlled during the acquisition of a tilted series of projections by a cooled slow-scan charge-coupled device (CCD) camera for 3D electron tomography (3D-ET) by fully digitized and automated TEM. A series of tilted projections were acquired for this experiment from −60° to 60°, with an image recorded every 2° to give a total of 60 images. A short exposure time (1.0 sec) was used to reduce the damage of the samples by irradiation. Once the acquisition of a tilt series was complete, the data were transferred to a workstation for fine-tuning of the alignments and for 3D reconstruction. These data were spatially aligned using a cross-correlation algorithm in IMOD software, and a 3D reconstruction was achieved by using a weighted back-projection of consecutive 2D slices by AMIRA 3.0.

Received: December 4, 2004
Published online: February 25, 2005

Keywords: gold · helical structures · nanotechnology · natural products · organic–inorganic hybrid composites

[1] A. Fu, C. M. Micheel, J. Cha, H. Chang, H. Yang, A. P. Alivisatos, *J. Am. Chem. Soc.* **2004**, *126*, 10832 – 10833.

[2] a) S. Yamada, T. Tasaki, T. Akiyama, N. Terasaki, S. Nitahara, *Thin Solid Films* **2003**, *438–439*, 70 – 74; b) S.-J. Park, T. A. Taton, C. A. Mirkin, *Science* **2002**, *295*, 1503 – 1506; c) J.-M. Nam, S.-J. Park, C. A. Mirkin, *J. Am. Chem. Soc.* **2002**, *124*, 3820 – 3821; d) E. Katz, I. Willner, *Angew. Chem.* **2004**, *116*, 6166 – 6235; *Angew. Chem. Int. Ed.* **2004**, *43*, 6042 – 6108; e) C. M. Niemeyer, *Angew. Chem.* **2001**, *113*, 4254 – 4287; *Angew. Chem. Int. Ed.* **2001**, *40*, 4128 – 4158; f) B. Yang, S. Kamiya, K. Yoshida, T. Shimizu, *Chem. Commun.* **2004**, 500 – 501; g) H. Matsune, N. Nakashima, N. Kimizuka, *Polymer Preprints, Jpn.* **2002**, *51*, 2435 – 2436.

[3] a) C. A. Mirkin, R. L. Letsinger, R. C. Mucic, J. J. Storhoff, *Nature* **1996**, *382*, 607 – 609; b) L. Josephson, J. M. Perez, R. Weissleder, *Angew. Chem.* **2001**, *113*, 3304 – 3306; *Angew. Chem. Int. Ed.* **2001**, *40*, 3204 – 3206; c) J.-M. Nam, S. I. Stoeva, C. A. Mirkin, *J. Am. Chem. Soc.* **2004**, *126*, 5932 – 5933.

[4] a) A. P. Alivisatos, K. P. Johnsson, X. Peng, T. E. Wilson, C. J. Loweth, M. P. J. Bruchez, P. G. Schultz, *Nature* **1996**, *382*, 609 – 611; b) J. J. Storhoff, A. A. Lazarides, R. C. Mucic, C. A. Mirkin, R. L. Letsinger, G. C. Schatz, *J. Am. Chem. Soc.* **2000**, *122*, 4640 – 4650.

[5] S. Connolly, S. N. Rao, D. Fitzmaurice, *J. Phys. Chem. B* **2000**, *104*, 4765 – 4776.

[6] a) M. Brust, D. Bethell, C. J. Kiely, D. J. Schiffrin, *Langmuir* **1998**, *14*, 5425 – 5429; b) Y. Kuwahara, T. Akiyama, S. Yamada, *Thin Solid Films* **2001**, *393*, 273 – 277; c) T. Sagara, T. Kato, N. Nakashima, *J. Phys. Chem. B* **2002**, *106*, 1205 – 1212.

[7] a) K. Tanaka, A. Tengeiji, T. Kato, N. Toyama, M. Shionoya, *Science* **2003**, *299*, 1212 – 1213; b) M. Shionoya, *Macromol. Symp.* **2004**, *209*, 41 – 50.

[8] K. Sakurai, S. Shinkai, *J. Am. Chem. Soc.* **2000**, *122*, 4520 – 4521.

[9] K. Miyoshi, K. Uezu, K. Sakurai, S. Shinkai, *Chem. Biodiversity* **2004**, *1*, 916 – 924.

[10] a) H. Okumura, Y. Kawaguchi, A. Harada, *Macromolecules* **2003**, *36*, 6422 – 6429; b) P. N. Taylor, M. J. O'Connell, L. A. McNeill, M. J. Hall, R. T. Aplin, H. L. Anderson, *Angew. Chem.* **2000**, *112*, 3598 – 3602; *Angew. Chem. Int. Ed.* **2000**, *39*, 3456 – 3458; c) A. Harada, *Acc. Chem. Res.* **2001**, *34*, 456 – 464; d) T. Michishita, M. Okada, A. Harada, *Macromol. Rapid Commun.* **2001**, *22*, 763 – 767.

[11] a) M. Numata, M. Asai, K. Kaneko, T. Hasegawa, N. Fujita, Y. Kitada, K. Sakurai, S. Shinkai, *Chem. Lett.* **2004**, 232 – 233; b) T. Hasegawa, T. Fujisawa, M. Numata, M. Umeda, T. Matsumoto, T. Kimura, S. Okumura, K. Sakurai, S. Shinkai, *Chem. Commun.* **2004**, 2150 – 2151; c) M. Numata, T. Hasegawa, T. Fujisawa, K. Sakurai, S. Shinkai, *Org. Lett.* **2004**, *6*, 4447 – 4450.

[12] a) J. J. Storhoff, R. Elghanian, C. Mucic, C. A. Mirkin, R. L. Letsinger, *J. Am. Chem. Soc.* **1998**, *120*, 1959 – 1964; b) M. Brust, D. Bethell, C. J. Kiely, D. J. Schiffrin, *Langmuir* **1998**, *14*, 5425 – 5429.

[13] D. J. Maxwell, J. R. Taylor, S. M. Nie, *J. Am. Chem. Soc.* **2002**, *124*, 9606 – 9612.

[14] R. Takahashi, T. Ishiwatari, *Chem. Commun.* **2004**, 1406 – 1407.

[15] Electron tomography (ET) is a useful technique for reconstructing an object from a series of projections acquired by TEM. Recent development of fully digitized and automated TEM has enabled us to achieve three-dimensional ET images, not only to determine the size and distribution of objects but also to provide information about the morphology of them on the nanometer scale. Three-dimensional structures were reconstructed by processing a series of projections through a combination of IMOD and Amira. See: a) J. Frank, *Three-Dimensional Electron Microscopy of Macromolecular Assemblies*, Academic Press, San Diego, **1996**; b) P. A. Midgley, M. Weyland, *Ultramicroscopy* **2003**, *96*, 413 – 431; c) J. R. Kremer, D. N. Mastronarde, J. R. McIntosh, *J. Struct. Biol.* **1996**, *116*, 71 – 76.

[16] This 1D alignment was reproducibly observed for Au nanoparticles with diameters of 2–20 nm, but not for those with a diameter of 250 nm.

